ELSEVIER

NeuroImage

www.elsevier.com/locate/ynimg
NeuroImage 37 (2007) 463–473

A neonatal atlas template for spatial normalization of whole-brain magnetic resonance images of newborns: Preliminary results

Kamran Kazemi,[a,b,*] Hamid Abrishami Moghaddam,[a,b] Reinhard Grebe,[a] Catherine Gondry-Jouet,[c] and Fabrice Wallois[a,d]

[a]*GRAMFC, Faculty of Medicine, University of Picardie Jules Verne, 80036 Amiens, France*
[b]*Faculty of Electrical Engineering, K. N. Toosi University of Technology, P.O. Box 16315-1355, Tehran, Iran*
[c]*GRAMFC, MRI Unit, Department of Radiology, North Hospital, 80056 Amiens, France*
[d]*GRAMFC, Neuropediatric Functional Explorations Unit, North Hospital, 80056 Amiens, France*

Received 18 January 2007; revised 30 April 2007; accepted 4 May 2007
Available online 10 May 2007

Commonly used brain templates are based on adults' or children's brains. In this study, we create a neonatal brain template. This becomes necessary because of the pronounced differences not only in size but even more importantly in geometrical proportions of the brains of adults and children as compared to the ones of newborns. The template is created based on high resolution T1 magnetic resonance images of 7 individuals with gestational ages between 39 and 42 weeks at the dates of examination. As usual, the created template presents two characteristics in a single image: an average intensity and an average shape. The normalization process to map subjects to the same space is done using SPM2 (Statistical Parametric Mapping) and its deformation toolbox. It consists of two steps: an affine and a nonlinear registration for global and local alignments, respectively. The template was evaluated by *(i)* study of anatomical local deviations and *(ii)* amount of local deformations of brain tissues in normalized neonatal images. The extracted results were compared with the ones obtained by normalization using adult and pediatric templates. It was shown that the application of our neonatal brain template for alignment of neonatal images results in a pronounced increase in performance of the normalization procedure as indicated by reduction of deviation of anatomical equivalent structures. The neonatal atlas template is freely downloadable from http://www.u-picardie.fr/labo/GRAMFC.

Keywords: Neonate; MRI; Spatial normalization; Template; Stereotaxic space

Introduction

Medical atlases are an important tool used in teaching and for inter-individual comparison and diagnostics of abnormal anatomical variations (Mazziotta et al., 1995). Since Brodmann (1909), the creation and use of brain atlases have been central for our understanding of brain anatomy variability. Brain atlases are built from one or more representations of brains (Toga and Mazziotta, 1996). They describe brain structure and function. Recent advancement in magnetic resonance (MR) imaging technology has provided the basis for the creation of numerous computerized brain atlases based on a statistically significant number of different MR images. For the construction of these atlases, templates and models have to be created to describe brain structure and organization (Thompson et al., 2000b).

There exists a high individual variability in brain morphology. So, before any inter- or intra-individual comparison can be performed, an image of a subject has to be spatially normalized to atlas coordinates called stereotaxic space. This procedure provides a common spatial framework to make statistical comparison between groups of subjects, to study intra- and inter-population morphological and functional variations. Warping a new image into a stereotaxic space is done using a template built from a certain number of brain images. The mean image model (template) for a group is created either by averaging the intensity, the shape or both (Guimond et al., 2000). Currently, the template created by the Montreal Neurological Institute (MNI) based on adult MR images is accepted as a standard by the International Consortium for Brain Mapping (ICBM). This template, named ICBM152, was generated by averaging 152 anatomical MRI after correction for overall brain size and orientation (Evans et al., 1993).

Increasing interest in neonatal structural and functional imaging (Bluml et al., 2004; Jones et al., 2004) has created a demand for a neonatal brain template. In studies involving adults, the subject's brain is normalized to the adult template derived from adult brains. However, the accuracy achieved by spatial normalization of neonatal or pediatric cerebral images using the adult template is questionable. Muzik et al. (2000) and Burgund et al. (2002) have conducted some studies in order to verify if there is a significant difference between the alignment results for images of children and adults brains using the adult template. These studies have demonstrated that if cerebral images of children are aligned using the adult template, there will be an increase in variation of anatomical landmark positions for individual images of children as compared for the same procedure for adult normalized images. Generally, normalizing an individual brain to a

* Corresponding author. GRAMFC, Faculty of Medicine, University of Picardie Jules Verne, 80036 Amiens, France. Fax: +33 3 22 82 79 63.
E-mail address: kamran.kazemi@u-picardie.fr (K. Kazemi).
Available online on ScienceDirect (www.sciencedirect.com).

1053-8119/$ - see front matter © 2007 Elsevier Inc. All rights reserved.
doi:10.1016/j.neuroimage.2007.05.004

template consists of two kinds of deformation, global affine transformation and local nonlinear deformation. Studies performed by Wilke et al. (2002) have shown that normalization of cerebral images of children using a pediatric template results in less nonlinear local deformation than while using an adult template. Hence, they created a pediatric brain template (CCHMC[1]) using cerebral images from children between 5 and 18 years old and proposed to use it for normalizing children images (Wilke et al., 2003).

Warping of neonatal cerebral images to an adult (or even pediatric) template is even more problematic than the alignment of pediatric images to an adult template. This is due to less anatomical similarity between neonatal and adult cerebral images. The most obvious differences are in head and brain sizes between neonates, children and adults. Moreover, there are age dependent differences in the proportion of brain region sizes due to growth (Gaillard et al., 2001). On the other hand, the process of brain maturation separates white matter tissue into two types: myelinated and non-myelinated. Non-myelinated white matter in neonates has a different intensity profile as compared to adult's white matter; it is dark in T1-weighted and bright in T2-weighted images (Ketonen et al., 2005).

To overcome the inaccuracies caused by using inappropriate templates for newborns, it has been proposed to use age dependent templates for growing subjects such as newborns (Gaillard et al., 2001). Dehaene-Lambertz et al. (2002) have created and used a specific template using T2 images of two young babies with the age of 3 months in order to determine which brain regions support language processing during the first months of life. For this purpose, they manually identified the anterior commissure (AC) and the posterior commissure (PC) in both subjects, aligned them manually according to these reference points, calculated the average image and finally smoothed it to generate a template.[2] In the method proposed by Prastawa et al. (2005) for model based neonatal brain segmentation, T1 and T2 templates have been created by averaging three affine registered neonatal images. They used these average intensity images to register a structural probabilistic atlas to the input image using only affine transformation. To the best of the authors' knowledge, the above two studies are the only ones which have aimed to create specific templates for young babies or newborns. However, these rest relatively preliminary and incomplete, presenting no evaluation concerning correctness and effectiveness of normalizing neonatal cerebral images using specific neonatal template.

In the here presented work, we developed a procedure for creation of atlas templates which we applied to create an atlas template of the neonatal brain using a set of high resolution T1-weighted MR images from a group of newborns with the gestational age of 39 to 42 weeks at the examination date. We also address the question of a need for different templates for different age groups of newborns.

The created template presents two characteristics: average intensity and average shape, both in a single image. In order to create the template, we initially select an image as reference. The reference image is positioned in a way that the AC is placed at the origin and the line connecting the anterior with the posterior commissure is in the horizontal plane. Then, in order to correct the position and global shape differences of all images in the data set, the affine registration is applied to them with respect to the reference image. In the next step, the registered images are nonlinearly normalized to the reference image using the method presented by Ashburner and Friston (1999). The average deformation is then applied to the normalized images. From these, the template is created by averaging. Finally, in order to reduce the bias effect of the reference image, we repeat the above process on the data set by using the created template as the reference.

In Materials and methods, we present the steps towards the construction of the geometric template. The created template and its evaluation results are presented in Results. Finally, the last section is devoted to conclusion and discussion.

Materials and methods

Subjects

Participants of the study have been 33 newborns of gestational age between 39 and 42 weeks at the date of MR examination (17 boys and 16 girls). All of them (except two images) were recruited from the university-hospital of Amiens-France during 3 years. Neonates were sedated in order to keep them motionless during the scan period, thus to reduce motion artifacts. This required additional care about respiratory depression, which might compromise the neonate's ability to maintain appropriate ventilation and oxygenation during the procedure. Their ears were protected by headphones and their body and head were snugly swaddled to ensure comfort throughout the MRI study. While in the scanner, all vital signs were monitored and a neonatal research nurse and pediatrician remained with the infant throughout the MRI study. All of the examinations have been performed for routine diagnostical purposes in the context of the clinical treatment of these newborns.

After reviewing of the MR images by a pediatric neuroradiologist, 14 subjects (8 girls and 6 boys) presenting no serious cerebral anatomical abnormalities were selected. From them, 7 subjects (4 girls and 3 boys) were selected to create the neonatal brain template and the 7 remaining images were used as cross-validation to evaluate the template. All the images used for template creation were acquired by General Electric 1.5 T scanner.

Data acquisition

Newborns were imaged with General Electric 1.5 T ($N=30$) and 3 T ($N=1$) scanners. The two remaining images were obtained by a Siemens 3 T MR scanner. All MR image acquisitions lasted less than 10 min. The structural 3D volumetric T1-weighted imaging sequence with 1.5 T scanner has had the following parameters: TR=10.1 ms, TE=2.208 ms and TI=500 ms. Each 3D volume consists of 512× 512 pixels for each slice which have been obtained from an acquisition matrix of size 256×256 (320×224 for one of the volumes) with 220 mm field of view (voxel size of 0.47×0.47×0.7 mm). The number of slices for axial acquisitions was 132, 140 and 152 and for coronal acquisitions 140, 152 and 164 in order to cover the entire head. The parameters for the General Electric 3 T scanner were: TR=12.62 ms, TE=4.25 ms, TI=400 ms, slices=108, axial acquisition matrix=512×256, data matrix=1024×1024 pixels for each slice, field of view=220 mm and voxel size=0.25×0.25×1 mm. Finally, the parameters for the Siemens system were: TR=1820 ms, TE=4.38 ms and TI=1100 ms, slices=160, coronal acquisition matrix=256×246, data matrix=256×256 pixels and voxel size=1×1×1 mm. The non-axial images were reoriented to the axial plane and all of the images were resliced to 0.47×0.47×0.47 mm cubic voxels.

[1] Cincinnati Children's Hospital Medical Center (www.irc.cchmc.org).
[2] www.unicog.org.

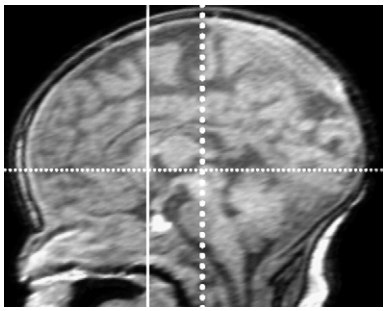

Fig. 1. Sagittal view of a newborn with gestational age of 41 weeks. The horizontal white line passing through AC and PC defines the y-axis. The vertical solid white line is the z-axis which passes through AC and the vertical pointed white line passes through PC.

Data pre-processing

All of the automatic image processing was done using Statistical Parametric Mapping (SPM2) software[3] and its deformation toolbox running in MATLAB. The only manual step in image preparation and analysis has been the determination of the AC and PC points, which has been performed by an expert for all images in the data set. During this procedure, the images have also been aligned along the main coordinate axes to correct for grossly different head positions in the scanner ensuring optimal starting estimates for the subsequent spatial normalization procedure.

The outputs of this step are images in which the AC–PC line corresponds to the y-axis in the horizontal plane and the AC point is the origin of the coordinate system. The z-axis is a vertical line that passes through the inter-hemispheric fissure and the AC point. Finally, the x-axis is a horizontal line at right angle to the y and z axes that also passes through AC (Fig. 1).

Template creation

Normalization procedure

The normalization of an individual image to a reference relies on a technique developed by Ashburner and Friston (1999), which has been implemented in SPM2 and its deformation toolbox. It is performed in two steps. In the first step, a 12-parameter affine transformation $A(\vec{x})$ including translation, rotation, scaling and shearing is used for a translation and linear deformation of the input images to the stereotaxic space as defined by the reference image. In the second step, a nonlinear deformation vector field $D(\vec{x})$ is used to match the subject to the target image on a regional level. This vector field is approximated using a set of $i \times j \times k$ cosine basis functions for deformation.

$$\vec{y} = A(\vec{x} + D(\vec{x})) \tag{1}$$

For the newborns in our application, we have selected a bounding box of $109 \times 134 \times 96$ mm^3 which contains the whole of the head. To obtain higher anatomical details as in the case of SPM for adult image normalization, we here smooth the source images with a 2 mm Full Width Half Maximum (FWHM) Gaussian kernel prior to normalization instead of the SPM one of 8 mm. The cutoff frequency for the cosine basis functions in the nonlinear step was reduced to 10 mm yielding 1430 basis functions (11 in x, 13 in y and 10 in z direction) in comparison to the default of 25 mm cutoff frequency used in SPM2.

Construction of neonatal template

The procedure proposed here, for the construction of neonatal template, shares some of the techniques used in the approach presented by Diedrichsen (2006) for the creation of an unbiased cerebellum template. Fig. 2c gives the block diagram of our method for the neonatal template creation process. Basically, it consists of three subsequent steps, namely: transformation and linear deformation, nonlinear deformation and averaging.

Transformation and linear deformation. In this first step, a medical specialist selects a subject as reference (I_R) whose head shape is symmetrical and has minimum deformation due to birth giving. Then, a 12-parameter affine transformation ($A_i(\vec{x})$) is applied to each individual image of the data set (I_i) in order to correct position and global shape differences with respect to the reference image:

$$I_i' = A_i(I_i), \quad i = 1, \ldots, N \tag{2}$$

Nonlinear deformation. The images resulting from the affine alignment are normalized to the reference image using a nonlinear deformation field D_i consisting of cosine basis functions to obtain the final normalized image I_i'':

$$I_i'' = D_i(I_i'), \quad i = 1, \ldots, N \tag{3}$$

To avoid a bias by the properties of one particular image, here the reference, an inverse transformation (T_i) is determined in the lower branch of Fig. 2c, which gives the mapping from the reference image to the corresponding subject images. The average $\overline{T}$ of these transformations (T_i) is calculated as follows:

$$\overline{T} = \frac{1}{N}\sum_{i=1}^{N} T_i \tag{4}$$

where N is the number of images in the data set. This new deformation is spatially unbiased with respect to the original group of individuals. In the final part of this step, the two branches are merged by applying this transformation $\overline{T}$ to each image I_i'' to obtain $\tilde{I}_i$:

$$\tilde{I}_i = \overline{T}(I_i''), \quad i = 1, \ldots, N \tag{5}$$

The deformation is computed with the help of the deformation toolbox.

Averaging. The average model is calculated by averaging all of the transformed images $\tilde{I}_i$. Finally, the average image is smoothed by a Gaussian kernel with 2 mm FWHM.

This procedure generates a template called first pass neonatal template (Fig. 2a). In order to further minimize the influence of the reference image, the template creation process is repeated by replacing the target image by the first pass neonatal template (Fig. 2b).

The major goal of the ongoing work presented in this paper is to create a template for neonates. Therefore, we apply the proposed approach for creating a geometric template (T_{39-42}). For the creation of the here presented version we used all of the images in the actual data set. Moreover, in an effort to investigate if it is advantageous to

[3] Welcome Department of Cognitive Neurology, University College London, UK.

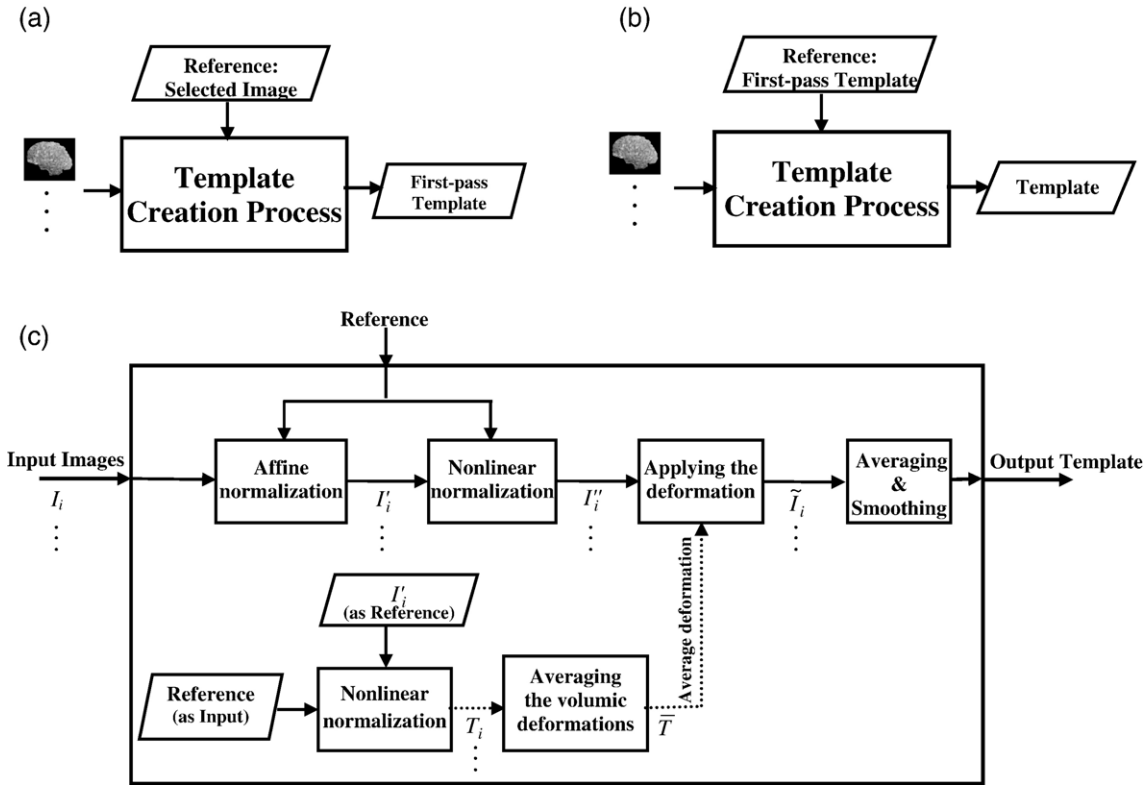

Fig. 2. Template creation procedure. (a) and (b) show the first and second stage of our algorithm for template creation. In these figures, the template creation process is presented as a black box with different inputs. (c) Block diagram of the template creation process.

create even more age differentiating templates, we used the above approach to create two templates for narrower ranges of age. In other words, we studied the application of two different templates ($T_{39–40}$ and $T_{41–42}$) which have been created separately from neonatal images with gestational age from 39 to 40 and 41 to 42 weeks, respectively.

Evaluation method

In order to evaluate the performance of our neonatal template in comparison with the existing ones, the neonatal images were first normalized to these templates and then the resulting images were compared with these templates. In more detail, to evaluate the anatomical precision of the spatial normalization of individual images using our neonatal template, we used two methods: *(i)* measurement of the spatial variation of similar anatomical structures after alignment, *(ii)* study of the displacement information stored in the deformation field obtained by nonlinear registration (Ashburner and Friston, 2000). For this purpose, the deformation field is translated into volumetric information which is used to analyze the shape differences.

Both methods of evaluation were applied in three different experiments. The first experiment was performed with the same images as already used for template creation. The second experiment was performed with the same images as in the preceding one but here by applying a 'leave-one-out' strategy. Finally, the third experiment was carried out with the cross-validation group of 7 additional images. For the second experiment (evaluation with leave-one-out method), we have chosen the image of one of the subjects in the data set as test image and built the template using the other images. By applying this method successively to all images of the data set, 7 templates were generated from 6 images each and evaluated by the 7th as the cross-validation image.

The same approach was used to verify if there is a need for further differentiation between the images of neonates of different gestational age by creating even more refined age related templates. Therefore, we subdivided the pool of our neonate images of gestational age of 39–42 weeks into the two subgroups 39–40 and 41–42 weeks and created as for the total the according age related templates ($T_{39–40}$ and $T_{41–42}$). Then we compared the normalization results given by the refined templates ($T_{39–40}$ and $T_{41–42}$) with the results given by using the $T_{39–42}$. These experiments gave an idea about the accuracy of normalization of neonate images due to different ages and the changes due to ongoing maturation when applying a relatively wide range template ($T_{39–42}$).

Anatomical measures

For the anatomical evaluation, we used predefined anatomical landmarks to quantify the variation of brain geometry which remains after normalization. This evaluation method has been used previously by Muzik et al. (2000) and Burgund et al. (2002) to compare the accuracy of the normalization of adult and children images to a common stereotaxic space as defined by an adult template. In our evaluation study, we examined possible differences between neonatal brain images after normalization into a common stereotaxic space by comparing *(i)* the AC and PC coordinates and *(ii)* the coordinates corresponding to a selected sulcus. The aim was to demonstrate that using a neonatal template for normalizing newborn images gives better results in term of accuracy as compared to using an adult or children template. We

used the same evaluation method to verify if there is further need for creation of even more age differentiating templates for neonates.

After image normalization, AC and PC of the normalized image should be located at the same position as the AC and PC of the template. Any deviation between corresponding points can be regarded as a measure for the error of the normalization. For this reason, we determined as well the mean of the distances between the AC of the template and the ACs in the normalized images as the corresponding mean for the PCs. Accordingly, the angle between the AC–PC line of the normalized images and the AC–PC line of the template was determined for the sagittal (θ) and the axial (φ) plane.

To study internal brain shape variation (Sowell et al., 2002) and to measure spatial spread of anatomical equivalent structures after alignment, we extracted a 3D curve characterizing the Sylvian fissure which is consistently identifiable even in premature neonates. The samples for the curve have been drawn manually from the coronal planes of the normalized images applying objective criteria. We then determined mean and standard deviation for all the curves obtained from the images normalized with a certain template. Again, this gives a criterion for the quality of the normalization: the smaller are mean and standard deviation (SD) the better match the images to the template.

To demonstrate the need for an appropriate template for normalization, the same process has been repeated for the test images which had been normalized by the newborn ($T_{39–42}$), adult (ICBM152) and pediatric (CCHMC) template, respectively.

Deformation

This evaluation aimed to study the amount of local nonlinear deformation needed to perform the normalization. A small total amount of these local changes indicates a small overall difference in shape between image and template, i.e. the similar are the two, provided the normalization result is reasonable.

After alignment of the subject's image to the template, we calculated the nonlinear deformation vector field as the distances between corresponding points in the template and the original image after affine normalization. The average length of all deformation vectors as well as the length of the biggest one has been determined. In order to study the influence of different templates on the results of normalization for newborn cerebral images, we compared these measures which have been calculated for different image–template combinations as listed in Tables 3A and 3B.

Results

Template creation

Fig. 3 shows the template created according to the method described in Materials and methods for term neonates with gestational age ranging between 39 and 42 weeks. The resulting template has a cubic resolution of $0.47 \times 0.47 \times 0.47$ mm^3. Its origin and axes are based on Talairach coordinates. The template is defined in a box sized $109 \times 134 \times 96$ mm^3 and contains the whole head including cerebrum and cerebellum. The lowermost axial cut was placed 8 mm below the cerebellum and the uppermost one at 1 mm above the head. The leftmost and rightmost sagittal cuts were placed at 2 mm distance from the head. Finally, the distances between the head and the first and last coronal slices were chosen to be 2 mm. To get a first overall confirmation of its anatomical validity we performed a semiautomatic segmentation of our template and determined for it the intracranial volume. The thus found value of 413.84 cm^3 is in good agreement with the one of 431.6± 29.43 cm^3 reported by Huppi et al. for the same age range (Huppi et al., 1998). Fig. 4 shows two templates with narrower age ranges (left: $T_{39–40}$ and right: $T_{41–42}$) which have been created by the same procedure.

Anatomical measurement

In this part of the evaluation study, we investigated the variability of the positions of predefined landmarks in the neonatal brain after normalization. Normalization was performed using neonatal (including $T_{39–40}$, $T_{41–42}$ and $T_{39–42}$), pediatric (CCHMC) and adult (ICBM152) templates. After the alignment, all of the images were successfully normalized to the common space defined by neonatal templates. However, the normalization was not successful for 8 images using the adult and 11 using the pediatric template from a total of 14 images in the data set. Most probably this has been caused by differences in intensity profile and object shape between the input images and the adult and pediatric templates which have been too big to allow for a successful matching.

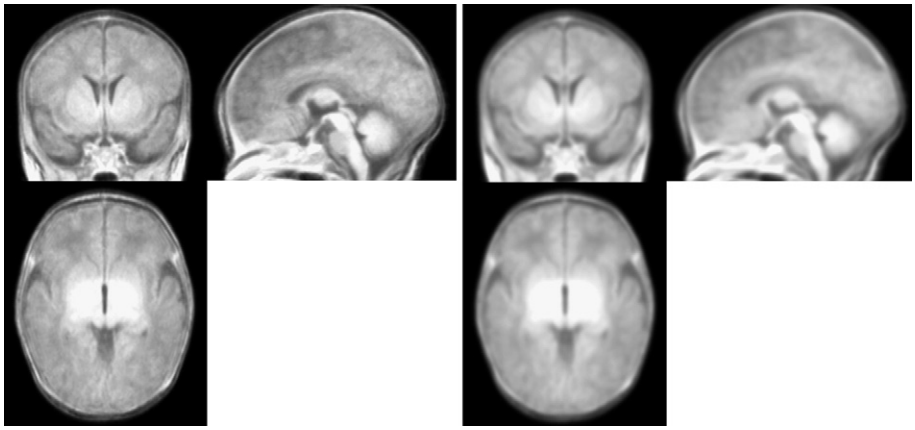

Fig. 3. Left: Neonatal template created from T1 MR images of newborns with gestational age between 39 and 42 weeks. Right: The template after smoothing with Gaussian filter (FWHM = 2 mm).

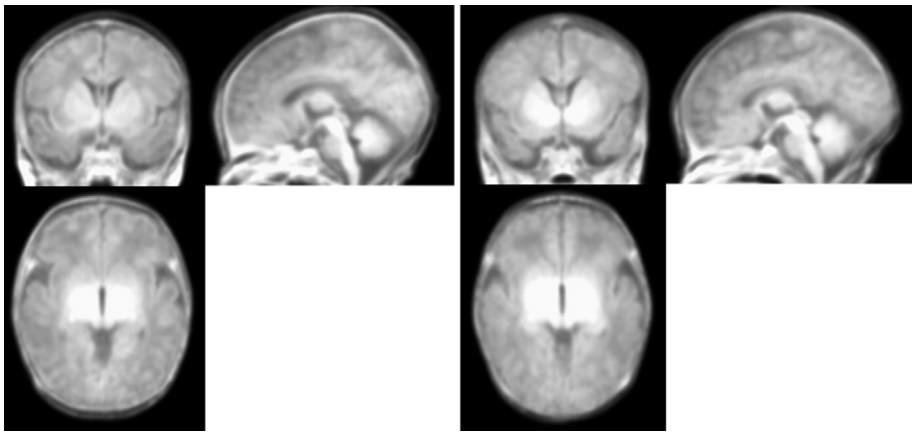

Fig. 4. Neonatal templates created from T1 MR images of newborns with gestational age between 39 and 40 weeks (left) and 41 and 42 weeks (right) after smoothing with a Gaussian filter with FWHM = 2 mm.

After normalization to the neonatal template the images were examined qualitatively and classified as identical by an expert (pediatric neuroradiologist). In the following subsections, we report the results of quantitative evaluation of the normalization with neonatal, pediatric and adult templates using the criteria described in Materials and methods.

Spread of AC and PC

Table 1A shows the data related to the variation of AC, PC and the angle of the AC–PC line with respect to their position and orientation in the space defined by different templates. The 3D coordinates of AC and PC in the normalized images of 14 participants were manually identified and used as landmarks. Section A in Table 1A shows mean and standard deviation of the distances between AC and PC in the normalized images and the corresponding points in each template. As illustrated, average errors in 3D positions of AC and PC with respect to their corresponding points in $T_{39–42}$ are at most 0.90 mm and 0.39 mm for all evaluated groups. On the other hand, when pediatric or adult templates are used, all of the images are considered as cross-validation. These values become 5.17 mm and 2.53 mm when the pediatric template is used and 5.11 mm and 4.91 mm when the adult template is used. Section B of Table 1A gives the average of the absolute deviation of the angles of the AC–PC lines in the normalized images with respect to the sagittal (θ) and the axial (φ) planes. The average absolute angle error is smaller than 1.84° for the sagittal plane and 0° for the axial plane. The according errors are 5.92° and 0.60° for application of pediatric templates and 1.94° and 0.64° for adult ones.

Table 1B presents anatomical measures related to the normalization by different neonatal templates as created from different age groups of neonates. In other words, this table gives a comparative evaluation of the error when specific neonatal templates (including $T_{39–40}$, $T_{41–42}$ and $T_{39–42}$) are used for normalization of neonates' images. The hypothesis behind this experiment is that the cerebral growth in newborns is naturally rapid and requires the use of different templates for different neonatal age ranges. The change in the total brain volume is approximately linear with an increase rate of 22 cm^3 per week for the newborns between 29 and 42 weeks (Huppi et al., 1998). More important in this context, there are also age dependent differences in growing of different brain structures (Gaillard et al., 2001). Anatomical measures were computed after

Table 1A
General neonatal template: error in location (mm) of AC and PC and in orientation (degrees) of the AC–PC line (mean ± SD)

	$T_{39–42}$	T_{CCHMC}	$T_{ICBM152}$
A.1. Distance from AC of the template			
Atlas samples	0.33 ± 0.22	–	–
Atlas samples (leave-one-out method)	0.39 ± 0.21	–	–
Cross-validation	0.90 ± 0.50	5.17 ± 1.59	5.11 ± 3.08
A.2. Distance from PC of the template			
Atlas samples	0.21 ± 0.18	–	–
Atlas samples (leave-one-out method)	0.39 ± 0.17	–	–
Cross-validation	0.27 ± 0.15	2.53 ± 0.75	4.91 ± 3.51
B.1. Absolute angle error (θ) of AC–PC line in sagittal plane			
Atlas samples	0.40 ± 0.64	–	–
Atlas samples (leave-one-out method)	0.20 ± 0.52	–	–
Cross-validation	1.84 ± 1.46	5.92 ± 3.62	1.94 ± 2.35
B.2. Absolute angle error (φ) of AC–PC line in axial plane			
Atlas samples	0	–	–
Atlas samples (leave-one-out method)	0	–	–
Cross-validation	0	0.60 ± 0.84	0.64 ± 0.91

Evaluation results related to the location of AC, PC and the angle of AC–PC line. The anatomical measures were computed after affine and nonlinear normalization of neonatal images to $T_{39–42}$, T_{CCHMC} and $T_{ICBM152}$. Section A: the mean and standard deviation of the distances between ACs and PCs in the normalized images and in the corresponding templates. Section B: the average absolute difference in the orientation of the AC–PC line in normalized images with respect to the same line in the templates in the sagittal (θ) and axial (φ) plane. In each section, the values reported in "Atlas samples" rows were obtained by using atlas samples as test images. Values reported in "Atlas samples (leave-one-out method)" were obtained by using atlas samples as test images but by applying a 'leave-one-out' strategy. Finally, values reported in "Cross-validation" rows were obtained by using additional 7 neonatal images as test images. It should be noted that among all 14 neonatal images, only 3 and 6 images were normalized successfully to T_{CCHMC} and $T_{ICBM152}$, respectively, and were considered as cross-validation subjects for these templates.

Table 1B
Age related templates: error in location (mm) of AC and PC and in orientation (degrees) of the AC–PC line (mean±SD)

	Neonates age range					
	39 to 40 weeks			41 to 42 weeks		
	T_{39-40}	T_{41-42}	T_{39-42}	T_{39-40}	T_{41-42}	T_{39-42}
A.1. Distance from AC of the template						
Atlas samples	0.16±0.22	–	0.35±0.32	–	0.12±0.20	0.32±0.12
Cross-validation	0.35±0.20	0.69±0.44	0.94±0.37	0.43±0.31	0.96±0.69	0.86±0.63
A.2. Distance from PC of the template						
Atlas samples	0.16±0.22	–	0.25±0.22	–	0.23±0.23	0.17±0.13
Cross-validation	0.23±0.23	0.36±0.24	0.25±0.16	0.33±0.22	0.22±0.31	0.30±0.15
B.1. Absolute angulation error (θ) of AC–PC line in sagittal plane						
Atlas samples	0	–	0.48±0.67	–	0	0.35±0.60
Cross-validation	0.36±0.62	1.18±1.13	2.18±0.75	0.83±1.05	1.77±2.50	1.39±1.97
B.2. Absolute angulation error (φ) of AC–PC line in axial plane						
Atlas samples	0	–	0	–	0	0
Cross-validation	0	0	0	0	0	0

Accuracy in identifying the AC and PC and the angle of the AC–PC line in neonatal MR images as a function of age related templates. Anatomical measures computed after affine and nonlinear normalization for neonates of gestational age from 39 to 40 (7 images) and 41 to 42 weeks (7 images). Values reported in each column are the errors due to normalization using the corresponding template. Section A: the mean and standard deviation of the 3D distances between AC and PC in the normalized images and the corresponding points in each template. Section B: the average absolute difference in the orientation of the AC–PC line in the normalized images with respect to the same line in the templates in the sagittal (θ) and axial (φ) plane.

affine and nonlinear normalization of 14 neonates, 7 used for creation of neonatal templates and 7 for cross-validation. We divided the subjects into two age categories 39–40 weeks (3 images for template creation and 4 images for test) and 41–42 weeks (4 images for template creation and 3 images for test) and computed the same anatomical measures as for Table 1A for each category using three different neonatal templates. For example, the first column of numbers in Table 1B shows the anatomical measures computed for the group of newborns of 39–40 weeks normalized to template T_{39-40}.

Location of the Sylvian fissure

As a general anatomical measure for the achieved normalization result, we evaluated the localization of a certain anatomical structure, the Sylvian fissure, in every normalized image (Fig. 5) as described in Materials and methods and compared it with the one

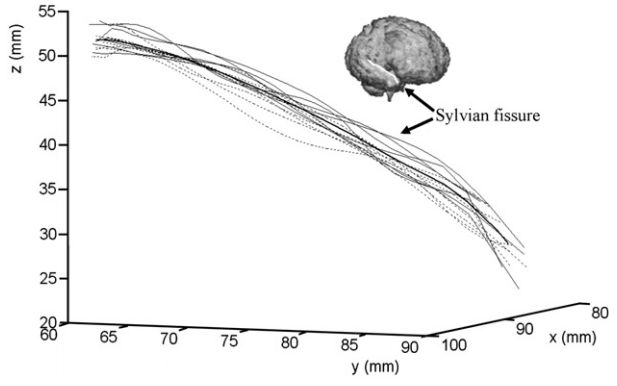

Fig. 5. 3D curves representing the location of the Sylvian fissures after normalization of the subjects to T_{39-42}. Thick curve: Sylvian fissure extracted from template T_{39-42}. Solid and dashed curves illustrate the Sylvian fissure for normalized atlas images and cross-validation images, respectively.

in the other normalized images and their target in the template. The characteristic curves extracted for this purpose should match as perfectly as possible. As a quantitative measure for the degree of overlap, we computed average and standard deviation of the distances between certain corresponding points in the curve of normalized images and the points in the template curve. The results are given in Table 2A, where Section A presents the comparison between the normalized images and Section B the comparison of the mean curve from the normalized images with the one of the template. Accordingly, in Fig. 5 the black thick curve presents the Sylvian fissure extracted from the template, the thin curves indicate the Sylvian fissures extracted from normalized atlas samples and the dashed curves are extracted from the cross-validation images. As indicated in the table, when different neonatal templates were used for normalization, the mean distance between the curves in normalized subjects and the curve in the template was 1.43 mm for atlas samples and 1.57 mm for cross-validation subjects. In contrary, when pediatric or adult templates were used for normalization of all subjects, the according mean distances became 3.74 mm and 4.64 mm, respectively. In Section B of Table 2A, the respective distances between the mean curve of the normalized images and the same curve in the corresponding template are shown. As illustrated, the maximum distance for atlas samples and cross-validation subjects was 1.07 mm, for T_{39-42}.

Table 2B focuses on the evaluation of the normalization error due to different gestational ages and related changes due to ongoing maturation. As mentioned in Materials and methods, specific age related neonatal templates (T_{39-40}, T_{41-42} and T_{39-42}) were created and used for normalization of according neonatal images and evaluated. Values reported in Section A are the mean and standard deviation of distances between the curves of normalized images and the curve in the corresponding template. These values are at most 1.44 mm and 2.19 mm for atlas samples and cross-validation subjects aged between 39 and 40 weeks. They are at most 1.43 mm and 1.61 mm as well for atlas samples and cross-validation subjects aged between 41 and 42 weeks. Furthermore, in Section B of the same table, the respective

Table 2A
General neonatal template: error in location (mm) of the Sylvian fissure (mean±SD)

	$T_{39–42}$	T_{CCHMC}	$T_{ICBM152}$
A. Mean distance from template curve			
Atlas samples	1.43±0.38	–	–
Atlas samples (leave-one-out method)	1.32±0.23	–	–
Cross-validation	1.57±0.50	3.74±1.07	4.64±2.60
B. Mean distance between template curve and mean curve in normalized images			
Atlas samples	0.52±0.12	–	–
Cross-validation	1.07±0.33	–	–

Improvement of anatomical overlap of the Sylvian fissure using neonatal template. Variation in location of the Sylvian fissure computed after affine and nonlinear normalization of neonatal images to $T_{39–42}$, T_{CCHMC} and $T_{ICBM152}$. Values reported for $T_{39–42}$ are the mean distances between the curves extracted from normalized images and the corresponding curve in the template. Values reported for T_{CCHMC} and $T_{ICBM152}$ are the mean distances between the curves in the normalized images and their mean curve. Section A: mean and standard deviation of the distance between the curves extracted from the normalized images and the curve in the corresponding template. Section B: distance between the mean curves extracted from normalized images and the curve in the corresponding template. In each section, the values reported in "Atlas samples" rows were obtained by using atlas samples as test images. Values reported in "Atlas samples (leave-one-out method)" were obtained by using atlas samples as test images but by applying a 'leave-one-out' strategy. Finally, values reported in "Cross-validation" rows were obtained by using additional 7 neonatal images as test images. It should be noted that among all 14 neonatal images, only 3 and 6 images were normalized successfully to T_{CCHMC} and $T_{ICBM152}$, respectively, and were considered as cross-validation subjects for these templates.

distances between the mean curve of the normalized images and the same curve in the corresponding template are shown.

Spatial deformation

After normalization to the neonatal templates, we calculated the deformation vectors which map every voxel of the template space into the corresponding voxel in the subject image. The average and maximal length of all deformation vectors provide a measure to study the effect of warping newborns to their specific templates.

Table 3A
General neonatal template: mean average and maximum length (mm) in deformation vector field (mean±SD)

	$T_{39–42}$	T_{CCHMC}	$T_{ICBM152}$
A.1. Mean of average length of deformation vector field for brain			
Atlas samples	1.91±0.43	–	–
Atlas samples (leave-one-out method)	2.20±0.64	–	–
Cross-validation	2.36±0.63	3.86±0.43	9.44±4.94
A.2. Mean of maximum length of deformation vector field for brain			
Atlas samples	5.52±1.27	–	–
Atlas samples (leave-one-out method)	6.27±1.65	–	–
Cross-validation	6.33±1.71	7.27±1.14	19.53±10.58
B.1. Mean of average length of deformation vector field for head			
Atlas samples	2.15±0.39	–	–
Atlas samples (leave-one-out method)	2.54±0.62	–	–
Cross-validation	2.45±0.63	4.23±0.80	11.13±6.39
B.2. Mean of maximum length of deformation vector field for head			
Atlas samples	8.14±2.19	–	–
Atlas samples (leave-one-out method)	9.51±2.76	–	–
Cross-validation	8.48±2.14	8.20±1.46	25.32±16.03

Mean and maximum length of deformation vectors computed after normalization of 14 neonatal images, of which 7 were used to create the neonatal templates and 7 for cross-validation. Values reported in each column are the average length of deformation due to normalization using the corresponding template. Section A shows the mean average and maximum length for brain tissues and Section B illustrates the mean average and maximum length for the head.

Table 2B
Age related templates: error in location (mm) of the Sylvian fissure (mean±SD)

	Neonates age range					
	39 to 40 weeks			41 to 42 weeks		
	$T_{39–40}$	$T_{41–42}$	$T_{39–42}$	$T_{39–40}$	$T_{41–42}$	$T_{39–42}$
A. Mean distance from template curve						
Atlas samples	1.22±0.12	–	1.44±0.17	–	1.28±0.18	1.43±0.47
Cross-validation	2.19±0.53	1.63±0.30	1.55±0.39	1.53±0.41	1.38±0.05	1.61±0.63
B. Mean distance between template curve and mean curve in normalized images						
Atlas samples	0.41±0.17	–	0.58±0.48	–	0.23±0.21	0.84±0.23
Cross-validation	1.97±0.60	1.12±0.43	1.27±0.39	0.71±0.40	1.05±1.88	1.17±0.72

Numerical evaluation of the distance between the Sylvian fissure in the normalized images and the template as a function of the age. The affine and nonlinear normalization of neonates of gestational age from 39 to 40 (7 images) and 41 to 42 weeks (7 images) were performed using age dependent templates. Values reported in each column are the mean distances between the sulcus in the normalized images and the sulcus in the corresponding template. Section A: mean and standard deviation of the 3D distances between the curves extracted from normalized images and the curve in the corresponding template. Sections B: distance between the mean curves extracted from normalized images and the curve in the corresponding template.

Table 3B
Age related templates: mean average and maximum length (mm) in deformation vector field (mean ± SD)

	Neonates age range					
	39 to 40 weeks			41 to 42 weeks		
	$T_{39–40}$	$T_{41–42}$	$T_{39–42}$	$T_{39–40}$	$T_{41–42}$	$T_{39–42}$
A.1. Mean of average length of deformation vector field for brain						
Atlas samples	1.97±0.58	–	2.11±0.54	–	1.61±0.29	1.77±0.32
Cross-validation	2.43±0.86	2.67±0.78	2.58±0.95	2.24±0.18	2.46±0.22	2.50±0.03
A.2. Mean of maximum length of deformation vector field for brain						
Atlas samples	5.98±0.84	–	6.52±1.51	–	4.48±1.04	4.77±0.02
Cross-validation	6.52±2.73	6.96±2.29	6.65±1.92	7.18±1.75	5.75±0.72	6.37±1.45
B.1. Mean of average length of deformation vector field for head						
Atlas samples	2.29±0.62	–	2.35±0.56	–	1.79±0.17	1.99±0.15
Cross-validation	2.44±0.79	2.77±0.72	2.51±0.84	2.59±0.20	2.61±0.14	2.8±0.24
B.2. Mean of maximum length of deformation vector field for head						
Atlas samples	8.91±2.08	–	9.17±2.79	–	6.50±0.87	7.37±1.61
Cross-validation	7.38±2.66	8.76±2.33	7.76±1.92	10.74±1.90	7.50±1.19	9.76±1.42

Evaluation of the mean and maximum length of the deformation vectors with respect to the age of the neonates. Neonates with gestational age from 39 to 40 (7 images) and 41 to 42 weeks (7 images) were normalized to different age related templates. Values reported in each column are the average length of deformation due to normalization using the corresponding template. Section A shows the mean average and maximum length for brain tissues and Section B illustrates the mean average and maximum length for the head.

For the 7 images that had been used for template creation, the average and maximum length of the deformation vectors were 1.91 mm and 5.52 mm for brain tissues according to $T_{39–42}$ (Table 3A). These values were 2.36 mm and 6.33 mm for the 7 cross-validation images. Similar results have been obtained using two other neonatal templates. We also calculated the deformation field for the whole head. The mean and maximal lengths of the deformation vectors were 2.15 mm and 8.14 mm for atlas images and 2.45 mm and 8.48 mm for cross-validations, respectively (Table 3A). Table 3B gives mean and maximum length of deformation vectors as resulting from normalization to different neonatal templates.

Furthermore, to illustrate the effect of this criterion in the case of well established treatment of adult images, we calculated the deformation needed to normalize adults to the adult's template. From this experiment the mean and maximum length of the deformation vectors for the adults have been determined to 2.58 mm and 6.64 mm for the whole head and 2.29 mm and 4.54 mm for the brain. In contrast, when we normalized neonates' images using the adult template, the corresponding values were 9.44 mm and 19.53 mm for the brain and 11.13 mm and 25.32 mm for the whole head (Table 3A).

Discussion and conclusion

In this paper, we presented an effort to build a neonatal brain template from high resolution T1 structural MR images. The within and between-slice spatial resolution was chosen to be 0.47×0.47 mm and 0.7 mm, respectively, to achieve a good spatial resolution regarding the small size of brain structures in newborns. Our data set was composed of 33 neonatal images of newborns of gestational age between 39 and 42 weeks. The template was created using 7 images and tested with another 7 images.

Normally, a much larger population would be desirable to ensure that the created template is of good quality and all individual biases are sufficiently reduced as this has been done in constructing the templates for adults and children. However, there are a number of specific problems with the creation of a neonates' template, which justifies our approach of a dynamically increasing population size:

The absence of images from volunteers: Adult and children templates were created by averaging a large number of MR images acquired from volunteers. Having volunteers among children and adults is possible under certain conditions. However, the situation is quite different for newborns. In our study, for obtaining newborn MRI images, we had to select among images which had been acquired from neonates for clinical purposes.

The difficulties to acquire MR images from neonates: As compared to MRI acquisition from adults or children, neonates require a controlled microenvironment and close monitoring to maintain respiratory and cardiovascular functions, body temperature, and fluid and electrolyte homeostasis. More importantly, neonates need to be sedated to minimize motion artifacts. This requires additional care about respiratory depression, which compromises the neonate's ability to maintain appropriate ventilation and oxygenation during the procedure. These limitations reduce drastically the number of available images of high quality of neurological healthy neonates and even more of complete ones.

The actual need of a neonates' template for normalization: The fact that 11 and 8 images (among 14) could not be normalized successfully to pediatric and adult templates, respectively, is itself a clear demonstration of the current difficulties for analyzing neonatal MRI cerebral images. The successful normalization of all 14 subjects with our neonatal template illustrates its promising performance for dealing with neonatal data. Therefore, we are convinced that already our actual template will result in more accurate normalization as compared to the use of pediatric and adult templates and that it can be useful for first applications and further developments towards automatic

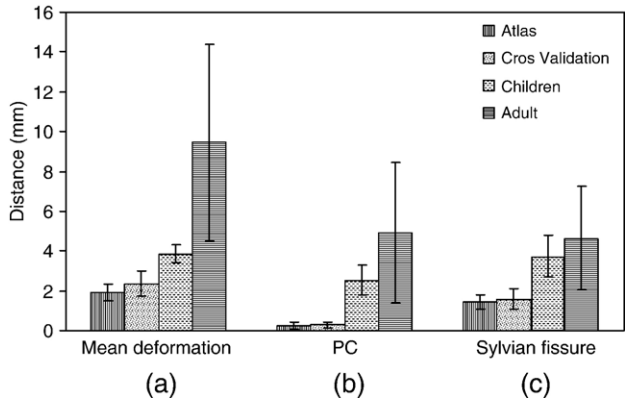

Fig. 6. Each of the three bar charts presents results achieved by applying the $T_{39–42}$ neonatal template (first two columns), the children template (third column) and the adult template (forth column), respectively. Bar chart (a) presents the mean deformation which results after normalization with the different templates, (b) the distance error for the position of the posterior commissure (PC) and (c) the overall positioning error of the Sylvian fissure. Normalization using our neonatal template results in moderate deformation and gives excellent exactness in PC position and good overall anatomical matching. In contrast, the use of the adult template results in more than four times higher deformation with relatively poor matching results indicated by much higher errors. Application of the children template gives better results than for the adults; however they are far from the neonatal ones.

segmentation of neonatal data. According to our knowledge, there is no similar template available for the scientific community and no evaluation has been made so far concerning the use of a specific neonatal template for normalizing neonatal images.

We are continuously working on augmenting the number of subjects in our data set. Thus, we developed an approach for template creation, which allows for permanent extension of the data set. Every new image will be entered in the procedure thus augmenting the number of subjects used for template creation.

The created template was evaluated and the achieved results were compared with those resulting from application of pediatric and adult templates for neonatal brain image normalization. The evaluation study was performed based on *(i)* variability in the location of predefined anatomical landmarks and *(ii)* amount of local deformations required for nonlinear normalization. Even so the amount of deformation obviously is not a measure for the goodness of a normalization result; it indicates nevertheless the degree of deformation necessary to achieve a certain similarity between image and template. The less deformation is needed the similar the image and template should be. From this point of view, the results in Table 3A show pronounced less average deformation for our general newborn template than for the two established ones. Anyway, interestingly enough comparing the established templates it turns out that the amount of deformation necessary with the adults ICBM152 template is more important and with a much higher SD than with the more appropriate pediatric CCHMC one (Fig. 6a).

The study of well defined landmarks has enabled us to determine a quantitative measure in terms of a distance from the expected AC and PC, which can be taken as a measure for the position error. Clearly, our study demonstrates a significant improvement in the location variability of predefined anatomical landmarks when images are normalized to our neonatal template compared to normalization with the standard pediatric and adult ones (Tables 1A, 1B and Fig. 6b). The study of a characteristic anatomical structure, the Sylvian fissure (Tables 2A, 2B and Fig. 6c), gives similar results. Also, application of specific neonatal templates results in less deformation and better matching. These results confirm the hypothesis that a specific neonatal template represents better the anatomical features of a specific population of newborns in comparison with different populations like children or adults (Thompson et al., 2000a).

If this is true, it might be worth to go even further and create templates which discriminate between neonates of different age. To investigate this possibility, we performed an additional study for which we selected the two age ranges of 39–40 and 41–42 weeks during which the growth process is sufficiently rapid for resulting in significant anatomical variations. A template was created for each group ($T_{39–40}$ and $T_{41–42}$) using appropriate subjects and images in the data set were aligned to their corresponding templates. Moreover, we aligned subjects in each group to the specific template of the other one and compared the results. The same evaluation measures were used for comparing the results of normalizing the subjects to each specific template.

Our finding from this experiment demonstrates only marginal improvement in normalization performance using relevant specific template for newborns with narrower age range (Tables 1B, 2B, 3B). However, in some cases the computed measures were contradicting this conclusion which probably was caused by the small number of test subjects used in the experiments. Obviously, a larger population size is required in order to confirm (or reject) the importance of this improvement.

In summary, in this paper we present a framework for construction and evaluation of a neonatal brain template from high resolution T1-weighted neonatal MR images. Our findings demonstrate the improved performance of the created template compared to pediatric and adult ones for normalization of newborns aged between 39 and 42 weeks. Our future works will be focused on enriching the created template by augmenting the number of samples and completing our study concerning the use of narrower age range templates.

Acknowledgments

This work was partially supported by Center for International Research and Collaboration of Iran (ISMO) under the grant number 83/20 and EGIDE France under the grant number 10118VG (Jundi Shapour scientific collaboration program) and by Iran's Telecommunication research Center (ITRC) under grant number 500/2535. We would like to thank Dr. Elna-Marie Larsson for providing high quality neonate MR images. We would like also to thank Dr. Marko Wilke and Dr. John Ashburner for their helpful comments and advises. Finally, we acknowledge Welcome Department of Imaging Neuroscience for providing SPM software that helped with the automatic normalization of the images.

References

Ashburner, J., Friston, K.J., 1999. Nonlinear spatial normalization using basis functions. Hum. Brain Mapp. 7, 254–266.

Ashburner, J., Friston, K.J., 2000. Voxel-based morphometry—The methods. NeuroImage 11, 805–821.

Bluml, S., Friedlich, P., Erberich, S., Wood, J.C., Seri, I., Nelson Jr., M.D., 2004. MR imaging of newborns by using an MR-compatible incubator

with integrated radiofrequency coils: initial experience. Radiology 231, 594–601.
Brodmann, K., 1909. Lokalisationslehre der Grosshirnrinde in Ihren Prinzipien Dargestellt auf Grund des Zellenbaues. Barth, Leipzig, Germany.
Burgund, E.D., Kang, H.C., Kelly, J.E., Buckner, R.L., Snyder, A.Z., Petersen, S.E., Schlaggar, B.L., 2002. The feasibility of a common stereotactic space for children and adults in fMRI studies of development. NeuroImage 17, 184–200.
Dehaene-Lambertz, G., Dehaene, S., Hertz-Pannier, L., 2002. Functional neuroimaging of speech perception in infants. Science 298, 2013–2015.
Diedrichsen, J., 2006. A spatially unbiased atlas template of the human cerebellum. NeuroImage 33, 127–138.
Evans, A.C., Collins, D.L., Mills, S.R., Brown, E.D., Kelly, R.L., Peters, T.M., 1993. 3D statistical neuroanatomical models from 305 MRI volumes. Proc. IEEE-Nucl. Sci. Symp. Med. Imaging Conf. 1813–1817.
Gaillard, W.D., Grandin, C.B., Xu, B., 2001. Developmental aspects of pediatric fMRI: considerations for image acquisition, analysis, and interpretation. NeuroImage 13, 239–249.
Guimond, A., Meunier, J., Thirion, J.-P., 2000. Average brain models: a convergence study. Comput. Vis. Image Underst. 77 (2), 192–210.
Huppi, P.S., Warfield, S., Kikinis, R., Barnes, P.D., Zientara, G.P., Jolesz, F.A., Tsuji, M.K., Volpe, J.J., 1998. Quantitative magnetic resonance imaging of brain development in premature and mature newborns. Ann. Neurol. 43, 224–235.
Jones, R.A., Palasis, S., Grattan-Smith, J.D., 2004. MRI of the neonatal brain: optimization of spin-echo parameters. Am. J. Roentgenol. 182, 367–372.
Ketonen, L.M., Hiwatashi, A., Sidhu, R., Westesson, P.-L., 2005. Pediatric Brain and Spine: An Atlas of MRI and Spectroscopy. Springer-Verlag, Berlin Heidelberg.
Mazziotta, J.C., Toga, A.W., Evans, A., Fox, P., Lancaster, J., 1995. A probabilistic atlas of the human brain: theory and rationale for its development. The International Consortium for Brain Mapping (ICBM). NeuroImage 2, 89–101.
Muzik, O., Chugani, D.C., Juhasz, C., Shen, C., Chugani, H.T., 2000. Statistical parametric mapping: assessment of application in children. NeuroImage 12, 538–549.
Prastawa, M., Gilmore, J.H., Lin, W., Gerig, G., 2005. Automatic segmentation of MR images of the developing newborn brain. Med. Image Anal. 9, 457–466.
Sowell, E.R., Thompson, P.M., Rex, D., Kornsand, D., Tessner, K.D., Jernigan, T.L., Toga, A.W., 2002. Mapping sulcal pattern asymmetry and local cortical surface gray matter distribution in vivo: maturation in perisylvian cortices. Cereb. Cortex 12, 17–26.
Thompson, P.M., Mega, M.S., Narr, K.L., Sowell, E.R., Blanton, R.E., Toga, A.W., 2000a. Brain image analysis and atlas construction. In: Fitzpatrick, M., Sonka, M. (Eds.), Handbook of Medical Image Processing and Analysis. SPIE Press, Bellingham, pp. 1066–1132.
Thompson, P.M., Mega, M.S., Toga, A.W., 2000b. Disease-Specific Brain Atlases, Book Chapter in: Brain Mapping: The Disorders. Academic Press.
Toga, A.W., Mazziotta, J.C., 1996. Brain Mapping: The Methods. Academic Press.
Wilke, M., Schmithorst, V.J., Holland, S.K., 2002. Assessment of spatial normalization of whole-brain magnetic resonance images in children. Hum. Brain Mapp. 17, 48–60.
Wilke, M., Schmithorst, V.J., Holland, S.K., 2003. Normative pediatric brain data for spatial normalization and segmentation differs from standard adult data. Magn. Reson. Med. 50, 749–757.